REPORT DOCUMENTATION PAGE

AFRL-SR-AR-TR-02-

0332

1. AGENCY USE ONLY (Leave blank)	2. REPORT DATE 02-28-2002	3. REPORT TYPE AND DATES COVERED Final Report 04/01/1998 – 08/31/2001

4. TITLE AND SUBTITLE	5. FUNDING NUMBERS
Time-Frequency Domain Memory and Processing	F49620-98-C-0022

6. AUTHOR(S)

David L. Huestis, Gregory W. Faris, and Eric A. Arons

7. PERFORMING ORGANIZATION NAME(S) AND ADDRESS(ES)	8. PERFORMING ORGANIZATION REPORT NUMBER
SRI International 333 Ravenswood Avenue Menlo Park, CA 94025	MP 02-004

9. SPONSORING / MONITORING AGENCY NAME(S) AND ADDRESS(ES)	10. SPONSORING / MONITORING AGENCY REPORT NUMBER
SRI International 333 Ravenswood Avenue Menlo Park, CA 94025	

11. SUPPLEMENTARY NOTES

12a. DISTRIBUTION / AVAILABILITY STATEMENT	12b. DISTRIBUTION CODE
Approved for public release, distribution is unlimited.	

13. ABSTRACT *(Maximum 200 Words)*

This report summarizes the results of a 3-year program of research on the physics and technology needed to develop high-performance optical memory and optical processing systems based on the concept called the stimulated photon echo (SPE). The research goals were investigation, demonstration, and improvement of signal strength and fidelity, architectures and algorithms, and materials properties for optical storage and in-memory processing. Key accomplishments were (1) development and demonstration of efficient algorithms for threshold discrimination and bit-error-rate reduction in retrieved binary images with large in-frame and frame-to-frame intensity variations; (2) demonstration and characterization of information storage in Erbium-doped crystals using 1.5-micron diode lasers compatible with fiber optic communications; (3) demonstration of improved phase-encoding schemes for in-memory temporal correlation of 1.5-micron pulse trains; (4) development of concepts for high-performance radar applications based on SPE optical memory for time-delay control of the transmitter array and in-memory image processing of the return signals; and (5) hosting the AFOSR Contractors' Meeting, "Optoelectronic Information Processing."

14. SUBJECT TERMS		15. NUMBER OF PAGES
optical memory, signal and image storage and processing, radar, holography, pattern recognition, optical communications		64
		16. PRICE CODE

17. SECURITY CLASSIFICATION OF REPORT	18. SECURITY CLASSIFICATION OF THIS PAGE	19. SECURITY CLASSIFICATION OF ABSTRACT	20. LIMITATION OF ABSTRACT
Unclassified	Unclassified	Unclassified	UL

NSN 7540-01-280-5500

Standard Form 298 (Rev. 2-89)
Prescribed by ANSI Std. Z39-18
298-102

20021031 021

CONTENTS

1.0 INTRODUCTION

The past 20 years of research, at SRI and elsewhere, on optical memories and in-memory processing based on the effects called the stimulated photon echo (SPE) and spectral hole burning have produced many technical successes and have accumulated a substantial foundation of scientific understanding of the underlying principles [Mo82, MB85, BBM86, KK87a, KK87b, XKH90, KBS92, SK92, SBK92, KXK93, SK93a, SK93b, SK95, SK96, SNP97, ZSK97, SK98, NSH98]. Very high storage densities are possible, 1000 gigabits per cubic centimeter or more. Single-channel data rates could be more than 10 gigabits per second, and even faster data throughput could be accomplished by massively parallel storage, retrieval, and in-memory processing of holographic images

Some key characteristics of SPE optical memory and processing have no analogues in existing computer technology. Each laser pulse associates an array of spatial pixels as having some implicit internal relationship. A time sequence of laser pulses might represent a similar internal correlation. This data representation, consisting of thousands of pixels in each of thousands of pulses, is quite different from conventional memory concepts of individually addressable elements, each containing a small number of bits (bytes, words, or even disk blocks) with no assumed or implicit relationship between them other than their serial bit addresses. This analysis, when combined with the continued exponential increases in performance of "conventional" technology, suggests emphasis on applications that need to store, retrieve, and process or analyze large collections of spatially or temporally related data. Such applications might include (1) temporal correlations for radar and signal intelligence and (2) spatial image storage, retrieval, and correlation. The GHz frame read and correlation rates of the SPE approach provide bit rates that are many orders of magnitude greater than any competing technology.

Because of its potential applications in the telecommunications industry, SRI's research program on SPE optical memory was supported initially (1986-1993) by the Nippon Telegraph and Telephone Corporation. Subsequent research, directed more toward military needs for data acquisition, storage, and processing, was funded by the U.S. Air Force and the Defense Advanced Research Projects Agency (DARPA).

This report summarizes the accomplishments of a 3-year program of research sponsored by the Air Force Office of Scientific Research (AFOSR). The long-term objective is development of very high-performance technology for short- to moderate-term storage and real-time analysis, correlation, and processing of large quantities of imagery and time-sequence data. The major sections of the report are (1) a description of the physical basis of SPE optical memory and processing, (2) a discussion of potential application areas, (3) a review of the work performed under the current contract, (4) an outline of prospective areas for future development, and (5) the program and abstracts for the contractors' meeting held at SRI in May 2000.
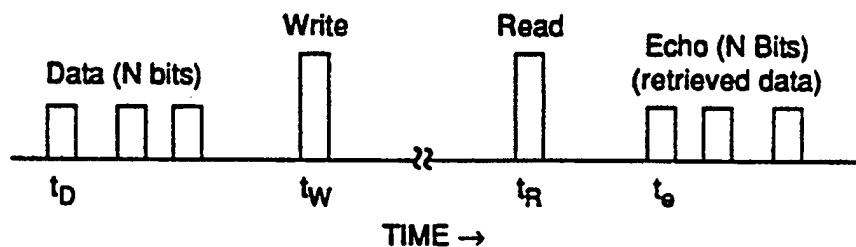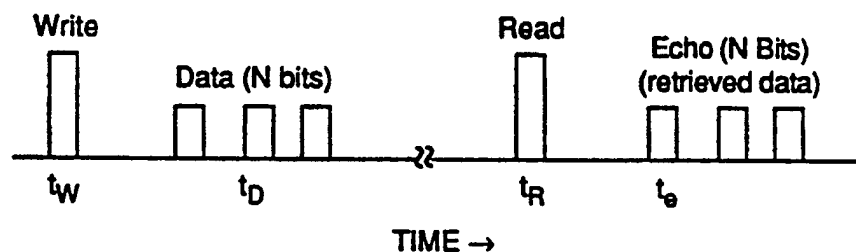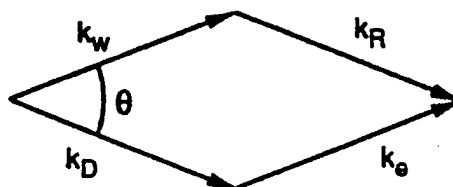
Figure 1. Temporal and angular sequence of processing with stimulated photon echo.

(a) Temporal schematic with time-reversal (equivalent to first-in-last-out [FILO] data memory).

(b) Temporal schematic without time reversal (equivalent to first-in-first-out [FIFO] data memory).

(c) One of the many possible relative directions of the write, data, read, and echo pulses.

3

2.2   Terabit Information Storage and Retrieval

To illustrate the storage of information in the time domain, we use a simple diagram to describe the storage and retrieval of, first, a single bit, and then, 10^7 bits of information, at a single spatial location. We use rare earth ion doped crystals for SPE. As an example, we consider $Eu:Y_2SiO_5$, which has an absorption frequency centered on 590 nm. At low temperatures (8 K to 30 K), the width of the absorption frequency of a single rare earth ion is very small (a few kilohertz); this width is also known as the homogenous width. However, the overall absorption width (or the inhomogenous width, as it is sometimes called) is much larger (many gigahertz) because the rare earth ions occupy a distribution of different sites and hence are exposed to different crystal fields. The ratio of inhomogenous to homogenous width, a parameter that directly reflects the number of bits of information that can be stored in a single micrometer-sized spatial pixel, is approximately 10^7 in $Eu:Y_2SiO_5$ crystals. We estimate that up to 10^{13} bits/cm^2 of information can be stored in this crystal. The individual ions in a crystal see the write and data pulses occurring at times $t_w = 0$ and t_D—not as two different pulses but rather as a complex pulse with a well-defined frequency Fourier transform. The information can be stored for many days at low temperatures in a $Eu^{3+}:Y_2SiO_5$ crystal.

To read the information, we need only excite the memory crystal at time t_R with a single laser pulse of the same colors as the data and write pulses. The read pulse causes the atoms to take the inverse Fourier transform of the frequency population modulation, and the result is a coherent emission or echo by the memory crystal at time $t_R + (t_D - t_w)$. The echo pulse emitted by the memory crystal mimics the data pulse train, and the serial data can therefore be retrieved. Furthermore, the coherent nature of the emitted signal from the memory crystal allows the entire signal to be captured by a single detector at a high signal-to-noise ratio (S/N). This angular dependence of the signal is in contrast to that of the two-photon memory, where the fluorescence radiates into all angles and results in a smaller S/N.

2.3   Parallel Storage

Storage of spatial images allows simultaneous access to multiple memory locations. This is one of the major advantages of the optical memory approaches over magnetic and semi-conductor memories; the stimulated echo approach is intrinsically parallel. Each of the data pulses shown in Figure 1 can represent not just one bit of information but potentially millions of bits of information because it is a spatial image with amplitude and/or phase modulation. We can use the spatial-temporal relationships to advantage in application to phased array antennas and synthetic aperture radar.

2.4   Temporal Correlation

Above, we discussed how the stored data waveform could be faithfully retrieved by exciting a micrometer-sized memory crystal with a simple, short, one-bit read pulse. However, if instead the read waveform is a more complicated waveform, it can be shown from Eq. (1) that the emitted echo no longer is a faithful replica of the data waveform but is proportional to the correlation between the data and read waveform.

5

2.5   Time-Frequency Domain Storage

Because the stimulated echo memory can store 10^{13} bits/cm^2, its true potential can be realized by storing information not only in the time domain but also in the frequency domain of a single pixel in the memory crystal. For example, as shown in Figure 4, the entire absorption frequency of the crystal memory can be subdivided into N frequency bins (colors), each of which can store several bytes of serial information. This storage can be accomplished by using a narrow linewidth laser and setting its frequency (color) to the center of one bin. The pulse sequence shown in Figure 1(a) now stores and retrieves the serial information at this frequency bin within a pixel. This can be used to advantage to increase storage capacity or for high rate processing. For example, many different filter functions or correlation signals can be stored in a single crystal. When the crystal is read with a broad band beam, appropriate convolution or correlation will be produced at each wavelength.
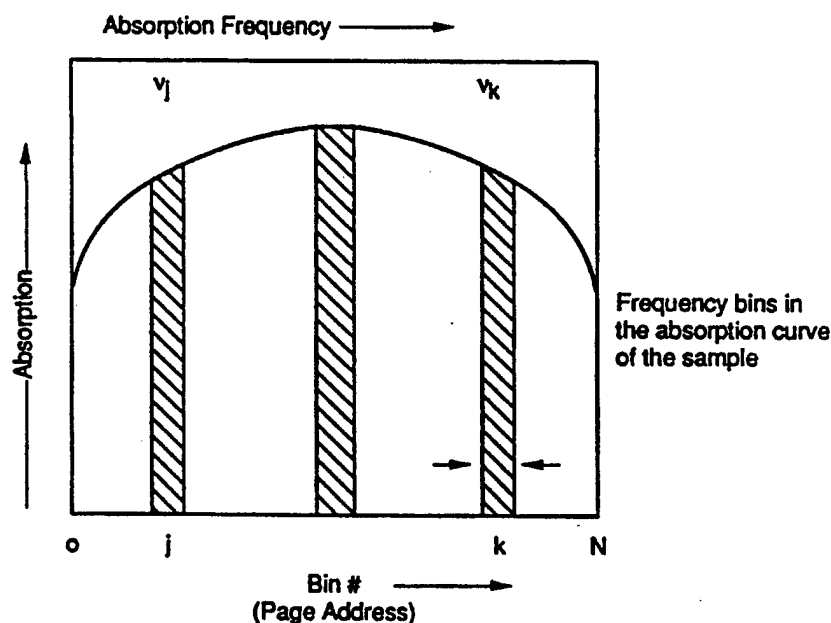
CM-330581-14

Figure 4. Division of absorption frequency spectrum into N frequency bins.

2.6   Rare Earth Ion Doped Crystals

Rare earth doped crystals, which are the best materials currently used in the stimulated echo approach, are one small class of materials among a large array of possible materials. However, in our opinion, only one class of materials has the highest potential for development for this application and is hence worthy of serious scientific investigation: rare earth ion doped crystals.

3.0   TECHNOLOGY APPLICATIONS

3.1   Computer Memory and Mass Storage

SPE optical memories were initially envisioned as providing exceptional speed and densities, on the order of 10 GHz per channel and 100 GB/cm^3. During the past 15 years, extensive laboratory and theoretical work on SPE optical memories has led to considerable advances in understanding of the underlying physical principles, material properties, and technology issues and questions that need to be resolved. However, over this same time period processor chips and mass storage devices in ordinary desktop computers (i.e., not just supercomputers) have already achieved performance levels approaching the SPE forecasts.

The greatest barrier to deployment of SPE optical memories is that its data manipulation characteristics do not map simultaneously to those of conventional computer components. For example, conventional computer processors and semiconductor random access memory (RAM) typically use word lengths of 8 to 64 bits, corresponding to the minimum and maximum size of a stored or retrieved information packet. A nominal access time is 1 ns, corresponding to 3×10^{10} bits/s (with parallel access). In contrast, SPE optical memories are most efficient with very large word sizes, say 10^5 bits, with an access time of 10 µs, or 10^{10} bits/s. Thus, even though the sustained data rates are comparable, and in spite of the potential large capacity of a SPE optical memory module, it is not simple to design a replacement RAM component. The short word lengths have been chosen because they roughly match the natural sizes of numbers, addresses, and instructions. Fast random access is important because the next memory location, from which to fetch an instruction or read or write a number, is not necessarily close to the last one accessed.

Existing mass storage devices (magnetic and optical) do have large word lengths, say 10^4 bits, slower access times, say 1 ms, and transfer rates approaching 10^9 bits/s. The current exponential improvements in the performance of high-speed "permanent" mass storage media and devices poses challenges for ideas for possible replacement devices based on "volatile" SPE optical memory technology. SPE still offers faster random access but suffers from cooling requirements. An intermediate application is perhaps that of cache memory, a large buffer that provides fast recall of recently read data without waiting for slow mass storage access. While this application is still attractive, it has received relatively little investigation. SRI had a short project from the Air Force in the early 1990s. Practical implementation requires matching the data manipulation characteristics and strategies of both RAM and mass storage devices.

Computer capacity is increasing by roughly a factor of 10 every 5 years. With the elapse of time, the potential thousand-fold advantage of SPE optical memories has been consumed. The future should be guided toward applications in which there are essential relationships between individual data items to be stored and manipulated. Such applications can benefit by the combination of high time-bandwidth product and parallel processing that the SPE approach provides. Examples might be long serial bit streams that we wish to search for characteristic shorter elements or two-dimensional images that we wish to store, retrieve, search, and process.

frame rate (30 Hz). In these experiments, the rate of image storage was limited by computer hardware and insertion loss from the SLM. In the course of this work we also developed algorithms for reduction in the bit error rate for extraction of page-formatted binary data.

The existing SPE approach can be extended to store, say, 10^5 images, each with 10^6 8-bit pixels. These could represent "objects" that we want to hunt for in an image or video stream. Each input image extracts a correlation echo signal from each of the stored images. The echo correlations exit the memory crystal with known angles and time separations. Using simple SLMs we have demonstrated operations at 30 Hz. 1-kHz SLMs are available commercially. After we learn how to use SPE technology as an effective SLM, framing rates of 30 kHz would become practical. Further development of these ideas for radar applications is described below.

3.4   Signal Processing

As illustrated in Figure 3 in Section 2.4 above, the SPE optical memory can perform general correlations and convolutions of temporal waveforms. This capability could be useful for encoding and decoding complex radar signals or encrypting and decrypting secure communications channels. It could also be used to perform signal analysis searching for characteristic patterns.

Here we will illustrate how to recognize and extract high-speed time domain information that might be buried in a large noise and jamming environment. The optical techniques are well suited to this problem because the solution may require hundreds or thousands of convolutions on a real-time basis between the received communication signal and a programmed set of target or reference waveforms (codes).

Two waveforms can be correlated easily by first storing a reference waveform, R_1, by exciting a small (micrometer-sized) sample with the reference and write waveform, at times t_R and t_w, respectively. The reference and write waveforms are produced by the modulator driver (MD) labeled MD_1 in Figure 5, which controls the reference/write waveform AOM (labeled AOMRW in Figure 5). The signal waveform, when it arrives at a later time, is first amplified and then modulates the laser via MD2 and AOMS, as shown in Figure 5. The received signal waveform pulse excites the same sample, causing it to radiate the echo waveform. The echo waveform is proportional to the correlation between the reference and received signal.

That the time of arrival of the target signal is not known can pose a serious problem for correlators, because the correlation must be done for all possible arrival times. However, using the SPE approach, the output correlation signal is obtained only when the correct target signal is present in the received signal. Therefore, this SPE correlator system is self-synchronizing over an infinite delay range. In other words, the target signal waveform can arrive at the correlator at any time delay relative to the reference pulses.

11

Because the reference waveform is stored in the sample for a long time, it can be correlated with another received signal waveform, S_2, at a later time. The sample radiates an echo signal that is proportional to the correlation between the reference waveforms and S_2. This process can be repeated for many received signal waveforms S_N ($N \approx 10^4$) at a rate of 10 to 100 kHz before a new copy of the reference waveform is needed to refresh the memory. It is also possible to store a different version of the reference waveform R_j in the same spatial location after every single correlation with a specific received signal waveform S_k.

In this particular example, we may need to correlate the received signal waveform S_i not only with one reference waveform R_1 but also with a set of perhaps 10^4-10^5 reference waveforms. This can be easily implemented as shown in Figure 2. We first divide the two-dimensional spatial surface of the memory crystal into N addressable locations, each a few square micrometers in size. In each of these spatial memory locations (called L_m), we store a reference waveform, R_m, by exciting the location L_m ($m = 1, \dots N$) with a reference waveform R_m and a write pulse, W.

Thus, before the arrival of the received signal waveform S_i, the sample is preloaded with N reference waveforms (matched filters), using the known reference waveforms shown in Figure 2. When the received signal waveform arrives, it is collimated and expanded so that it excites all the spatial memory locations simultaneously, with the result that each spatial memory element L_m performs a correlation between S_i and R_m and emits an echo that is proportional to this correlation. The echo emission from each spatial element can be imaged on a single photodetector P_m in a two-dimensional array. Therefore, N correlations between S_i and R_m ($m = 1, \dots N$) can be performed simultaneously and detected separately. By detecting the peak of the correlation signal of each of the N pixels of the photodetector, we can find the best matched reference waveform with the received signal input.

The straight solid line in Figure 6 shows the empirical local threshold used in this analysis:

$$T(I_{0ave}, I_{1ave}) = \tfrac{2}{3}(I_{0ave} + 11\sqrt{I_{0ave}}) + \tfrac{1}{3}(I_{1ave} - 11\sqrt{I_{1ave}})$$

Also shown by the straight dashed line in Figure 6 is the predicted "best threshold" calculated by solving equation d(BER(T))/dT=0, where

$$BER(T) = \tfrac{1}{2}\left[\int_{T}^{\infty} f_0^{\mu\lambda}(I)dI + \int_{0}^{T} f_1^{\mu\lambda}(I)dI + \right]$$

This threshold can be represented approximately by

$$T(I_{0ave}, I_{1ave}) = 1.2\,I_{0ave} + 0.18\,I_{1ave}$$

The new algorithm is useful for fast and reliable extraction of page-formatted binary digital data. The advantages of the algorithm include a low raw-bit-error rate, fast extraction speed, the use of a simple and density-efficient coding scheme, and large tolerance to a change of S/N. We used this algorithm to analyze shot-noise-limited binary data that had large interpage and intrapage intensity variations and obtained an improvement in the bit-error rate of 3 to 4 orders of magnitude compared with that in a single-threshold-detection scheme.

4.2   SPE Optical Memory at 1.5 microns

Early in the project we set up an experiment to store data in the 1.5 μm region by using a modular architecture, with connections between modules made by optical fibers. The storage material chosen for the demonstration is crystalline $Er^{3+}:Y_2SiO_5$ (0.005 atomic % and 7 mm thick). Optical information is stored in the $^4I_{15/2}$ - $^4I_{13/2}$ transition of the crystal, which has two optically equivalent sites, one at 1.5364 μm (site 1) and the other at 1.5388 μm (site 2). Each optical site has an inhomogeneous broadening of ~ 1 GHz. To increase the length of a data string that can be stored each time (which is determined by the phase memory time of the transition), we place the sample between two permanent magnets with a magnetic field (~ 3 kilogauss) perpendicular to the optical beam axis. Under this condition, the two-pulse echo intensity at both sites was found to decrease by three orders of magnitude over a pulse separation of ~ 110 μs, which corresponds to a phase memory time of ~ 140 μs. Using a storage cell of 0.8 mm diameter, 1020 bits of data were stored and recalled in a 40 -MHz frequency channel.

We also estimated the raw bit error rate (BER) of the unit by storing the same data string repeatedly for 100 times and plotting the intensity distributions of 0's and 1's. A total of 35,700 bits of data are used here and the two distribution curves are clearly separate, suggesting that a single threshold can be used to determine the state of each bit without generating an error bit.

15

set consisted of 120 bits each of 150-ns duration. The search code consisted of a 40-bit section from the complete data set. Five trials were run, with the start of each search code shifted 20 bits from the previous run. This corresponds to a time shift of 3 μs. The total time delay over the five trials was 12 μs.
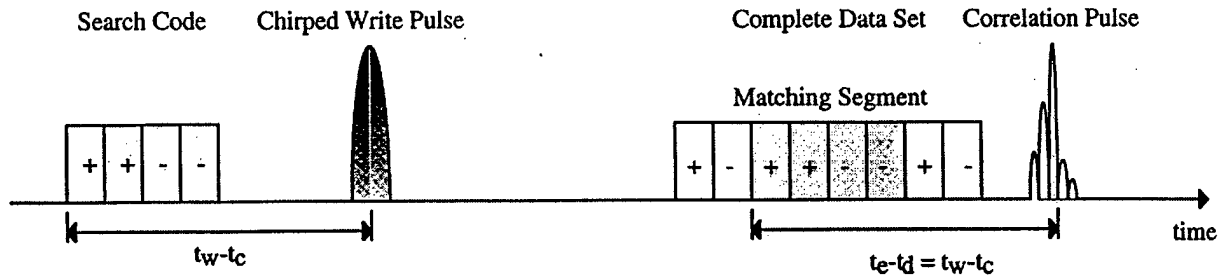
Search Code   Chirped Write Pulse   Complete Data Set   Correlation Pulse

Matching Segment

t_w-t_c $t_e-t_d = t_w-t_c$ time

Figure 8. Schematic Representation of Pulse Train Sequences

Figure 9 shows the results from the five runs. The correlation peak shifts in time by 3 μs as expected. Due to the short dephasing time in Er:YSO, the strength of the correlation peak decreased exponentially with increasing delay. This could be overcome by a compensating exponential amplification of the search bits and/or the complete data set.
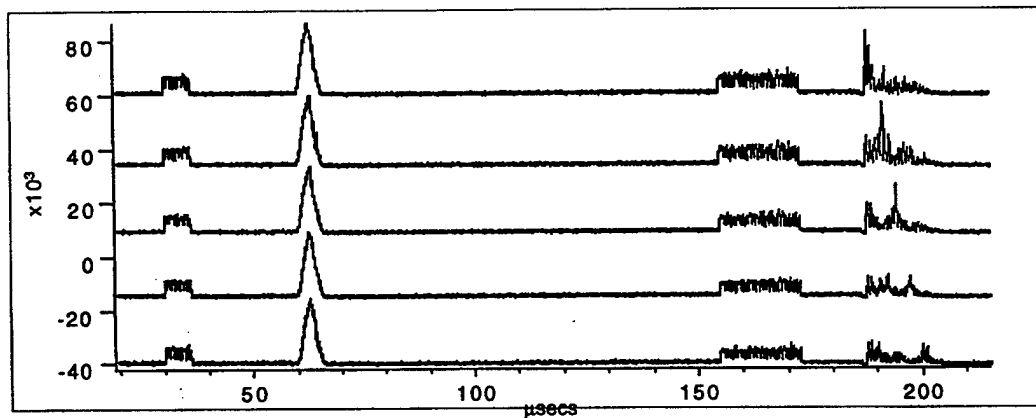
Figure 9. Experimental Correlation Signals

Previous methods used amplitude modulated bitstreams with random phase modulation to enhance correlation. This approach requires precise timing in the introduction of the phase information between the search code and the unknown data set. The current method encodes the bitstream as a binary phase modulation on a constant amplitude envelope. Therefore, no *a priori* knowledge of the timing of the unknown data stream is required for good correlation.

17

$K(\theta,\phi,z,x',y',t')$, is programmed using the conjugate or time-reversed x-y-t images used to illuminate the target scene. A similar approach can be used for passive direction finding and signal intelligence.

For synthetic aperture radar applications, a third SPE crystal would be used to coherently combine multiple scenes as the platform moves or as the target moves against a stationary background.

Although all these ideas require significant further research and development, they offer the potential for significant reductions in weight and improvements in performance over previous electronic and photonic approaches. These are demanding applications that need fast space-time processing. They are naturals for the SPE technology because the data necessarily have implicit bit-to-bit relationships in space and time. In addition, they are of strong AF/DOD interest and are not likely to be developed commercially.

4.5   Contractors' Meeting

On 25, 26 May 2000, SRI International hosted an AFOSR Contractors' and Grantees' Workshop on "Optoelectronic Information Processing." Thirty leading researchers made presentations. The meeting agenda and presentation abstracts are included as an appendix to this report. A compact disk containing the presentation materials is available.

6.0 MISCELLANEOUS

6.1 Personnel Supported

David L. Huestis

Gregory W. Faris

Eric A. Arons

Ravinder Kachru (left SRI)

Xiao-An Shen (left SRI)

Yu-Shen Bai (left SRI)

6.2 Publications

X. A. Shen and R. Kachru, "All-Optical Dynamic Memory for Fiber Communications," SPIE 3531, 11-15 (1998).

D. Nguyen, X. A. Shen, D. L. Huestis, and R. Kachru, "Algorithm for Extraction of Page-Formatted Binary Digital Data," Appl. Opt. 37, 8215-8218 (1998).

6.3 Interactions/Transitions

SPIE Annual Meeting, June 1997, San Diego, CA

Spectral Hole Burning Workshop, February 1999, Boseman, MT

Presentation at DARPA, February 2000, Arlington, VA

Presentation at NSA, February 2000, Ft. Meade, MD

AFOSR Contractors' Meeting, May 2000, Menlo Park, CA

6.4 New Discoveries/Inventions or Patent Disclosures

D. L. Huestis, "High Performance Control of Phased Array Radar Transmission," Invention Disclosure No. 4230-1, (SRI International, May 2000).

D. L. Huestis, "High Performance Phased Array Radar Receiver Analyzer," Invention Disclosure No. 4231-1, (SRI International, May 2000).

D. L. Huestis, "High Performance Direction Finding and Signal Intelligence," Invention Disclosure No. 4232-1, (SRI International, May 2000).

D. L. Huestis, "Phased Array Synthetic Aperture Radar," Invention Disclosure No. 4233-1, (SRI International, May 2000).

6.5 Honors/Awards

Ravinder Kachru was elected as a Fellow of the Optical Society of America (1998)

David L. Huestis is a fellow of the American Physical Society (1990)

SK96   X. A. Shen and R. Kachru, "Experimental Demonstration of Impulse-Equivalent Time-Domain Optical Memory," Opt. Lett. **21**, 2020 (1996).

SK98   X. A. Shen and R. Kachru, "All-optical dynamic memory for fiber communications," Proc. SPIE **3531**, 11-15 (1998).

SNP97   X. A. Shen, A.-D. Nguyen, J. W. Perry, D. L. Huestis, and R. Kachru, "Time-Domain Holographic Digital Memory," Science **278**, 96 (1997).

XKH90   E. Y. Xu, S. Krö ll, D. L. Huestis, R. Kachru, and M. K. Kim, "Nanosecond Spatial Image Processing Using Stimulated Echoes," Opt. Lett. **15**, 562 (1990).

ZSK97   Y. Zhang, X. A. Shen, and R. Kachru, "Observation of photon echo in Er^{3+}:YAG at 1.527 μm," Opt. Lett. **22**, 1068-1070 (1997).

ZT94   H. Zmuda and E. N. Toughlian, Eds., *Photonic Aspects of Modern Radar* (Artech House, Boston, 1994).

APPENDIX A

AFOSR CONTRACTORS' MEETING AGENDA AND ABSTRACTS

AFOSR Contractors and Grantees Workshop

SRI International, Menlo Park, California
25, 26 May 2000

25 May 2000

08:15   Kent Miller, AFOSR, Welcome

VCSELs, Quantum Devices

Quantum Computing

12:30 – 13:30 Lunch

12:00 – 13:00 Lunch

Signal Processing, Data Retrieval, Target Recognition

16:00 *Summary – Discussion of Goals and Future Directions*

Advanced Coherent Transient Systems and Devices

Wm. Randall Babbitt
Department of Physics, EPS Building 264
Montana State University, Bozeman, MT 59717-3840
babbitt@physics.montana.edu

The ability of frequency selective materials and structures to perform complex spectral and spatial filtering can be exploited via spectral-spatial holographic (SSH) techniques and adapted to the needs of high bandwidth, high performance processing systems. SSH time-space image processing systems can process time-space signals with bandwidths of 10GHz to 1THz and time-space bandwidth products of over 1,000,000,000. SSH multi-dimensional processors can perform the equivalent of more than a 10^{12} floating point operations (a complex valued 10000x1000x1000 correlation, for instance) every microsecond. Potential applications include true-time delay processors, multi-dimensional pattern recognition and associative memory, and code division multiplexing and routing. The objective of our AFOSR program is to explore both the physics and engineering issues in the development of SSH processors. Specifically, issues of efficiency, bandwidth, dynamic range, adaptive learning, modulation coding, multiplexing, and overall system performance are being investigated, as well as demonstrations of the concept of continuously programmed continuous processing, which enables currently available materials to be used in high performance systems.

Research Review of activities in the Center for Multidisciplinary Optical Switching Technology (MOST) at UCSB

John Bowers, Dan Blumenthal, Larry Coldren, Steve Denbaars,
Art Gossard and Nadir Dagli
University of California at Santa Barbara
bowers@ece.ucsb.edu

We review the research in optical switching technology in the DARPA MURI MOST Center program at UCSB. The center brings together a multidisciplinary team of researchers involved in semiconductor growth and processing, photonic and electrical integrated circuits, photonic packet switching technologies and network protocols and algorithm. Advances in VCSEL laser technology, integrated switch structures, fast wavelength conversion and optical packet routing and buffering will be covered.

Fabrication and Demonstration of a WDM, ATM, Multicast Switch

Fow-Sen Choa
University of Maryland, Baltimore County
choa@umbc.edu

We report our work on the implementation of an optical packet backbone switch. We design and fabricate switch components including: frame synchronizers, frame delineation units, frame header over-writing units, wavelength converters, frame concentrators, and all optical buffer memories independent of payload format or bit-rate. New materials and device structures have been identified through the process. We will report them in the meeting.

Selectively-Oxidized Microcavities and Quantum Dot Active Regions For Low-Threshold VCSELs and Controlled Spontaneous Lifetimes

D.G. Deppe
Microelectronics Research Center
Department of Electrical and Computer Engineering
The University of Texas at Austin, Austin, Texas 78712
deppe@mail.utexas.edu

Selective oxidation is a powerful processing technique to achieve small optical modes in a Fabry-Perot microcavity. The optical confinement is due to the (stepped) optical mode density of the planar Fabry-Perot microcavity modified by the intracavity aperture. When combined with quantum well active regions, this apertured-microcavity can be used to fabricate ultralow threshold VCSELs with threshold currents of 10's of microamps. Quantum wells, however, suffer from carrier diffusion, which limits their usefulness for very small oxide apertures. To overcome this limitation, quantum dots can be used in place of quantum wells to make possible electronic confinement in selectively oxidized apertures with micron dimensions. The resulting mode and electronic confinement are sufficient for the observation of the Purcell effect in modifying the quantum dot spontaneous lifetime. In this talk we will describe ultralow threshold lasing characteristics of selectively oxidized VCSELs, novel quantum dot emission characteristics extending laser operation to 1.3 μm wavelength, and controlled spontaneous lifetimes in which the lifetime of quantum dot emitters are shortened due to cavity confinement by a factor of ~2.5.

Programmable Meso-Optics with Resonant Near-Field Nonlinear Nanostructures

Yeshaiahu Fainman
Department of Electrical and Computer Engineering, 0407
University of California at San Diego
fainman@ece.ucsd.edu

This presentation focuses on the application of artificial dielectric materials to implement optical components with multifunctionality in polarization, color, electrical programmability and enhanced optical nonlinearity. We first review the progress in developing modeling tools for accurate analysis of periodic and nonperiodic meso-optic nanostructures, including near-field optical interactions, using the FEA, RCWA, and FDTD methods. These tools are applied to study several example devices, include form birefringent nanostructures, form birefringent multilayer structures, polarization selective photonic crystals, and a nanostructured electro-optic modulator. We also investigate the interaction of ultrashort laser pulses with artificial dielectric nanostructures, including a structure which exhibits near-field localization or concentration of the field, enhancing nonlinear optical phenomena. Finally, we discuss the advantages of artificial dielectric nanostructures-flexibility in the choice of materials and compatibility with standard microfabrication techniques- which enable easy integration with other photonic devices such as VCSELs, MQW modulators, and photodetectors.

Broadband Materials in the Region 800 nm for Spectral Hole Burning Applications

A. A. Gorokhovsky
The College of Staten Island and Graduate School of CUNY
2800 Victory Blvd.
Staten Island, NY 10314
gorokhovsky@postbox.csi.cuny.edu

Our research is directed toward the development and characterization of novel optical materials for optical hole-burning frequency and time-domain storage and processing applications. To characterize and compare different potential hole burning materials, we determined several material parameters, including the low-temperature cross-section of optical transition, the excited state optical lifetime, the inhomogeneous and homogeneous linewidths, the hole lifetime, the quantum yield of hole burning, and some others. The materials under investigation are comprised of three different groups with actual optical transitions in the spectral region 800 nm. The first group includes organic compounds naphthalocyanine and octabutoxy phthalocyanine embedded in different polymer hosts. Another group represents metalloorganic compounds, specifically Tm^{3+} β-diketone tris chelates of thulium blended in a poly (methyl methacrylate) matrix. The third group represents very hard inorganic materials - diamond and diamond-like carbon films doped with Si other ions. These three groups of materials possess an extremely wide range of optical properties that make them excellent candidates for investigation for the use in storage and processing applications involving spectral hole burning. Specifically, the first and second groups feature extremely broad bandwidth (up to 10 THz) and are prospective candidates for ultrafast applications and the third group represents prospective materials for high temperature (around 77 K) applications.

Dark Resonances in Spectral Hole Burning Materials

Philip Hemmer
AFRL/SNHC
Hanscom AFB, MA 01731
hemmer@plh.af.mil

Raman dark-resonances are being studied in spectral hole burning materials for a variety of applications ranging from high temperature spectral-hole-burning memories to optical aberration correction to quantum computing. The results of demonstration experiments performed in atomic vapors and Pr doped Y_2SiO_5 will be reviewed first. Next the materials requirements for specific applications will be outlined and candidate materials will be discussed. Finally, preliminary results will be presented on materials currently under study.

Integrated Devices for Terabit per Second 1.3 and 1.5 Micron WDM/TDM Network Applications

Prem Kumar
Northwestern University
kumarp@delta.ece.nwu.edu

Over the past several years we have been pursuing a research program to develop and demonstrate novel, compact, integrated, opto-electronic and optical devices for use in the emerging ultrahigh-speed WDM and TDM optical networks. We will present our recent accomplishments and the near-term goals.

The Application of Parallel Information- and Communication-Theoretic Methods to Storage and Imaging

Professor Mark A. Neifeld
Electrical and Computer Engineering Department
Optical Sciences Center
University of Arizona
Tucson, AZ 85721
neifeld@ece.arizona.edu

Volume optical storage systems require highly parallel interface processing for important tasks such as signal detection and error decoding. Our study of these interface requirements has resulted in powerful information- and communication-theoretic methods for use within the volume storage environment. Recently we have begun to extend these methods for application to other highly parallel scenarios. This presentation will discuss results from our work in parallel coding and signal processing and some extensions to problems in imaging and image processing.

Electrically Tunable Semiconductor Optical Delay Lines

Thomas R. Nelson, Jr., Ph.D.
U.S. Air Force Research Laboratory
Sensors Directorate, Electron Devices
Area B, BLDG 620, RM NE2-G8
Wright-Patterson AFB, OH 45433-7322
Thomas.Nelson@wpafb.af.mil

It is now well-established that pulses incident at either the long- or short-wavelength bandedge resonances of a Distributed Bragg Reflector (DBR) mirror experience appreciable decreases in their group velocity, leading to a time delay in transmission. Growing InGaAs quantum wells in the GaAs layers of a GaAs/AlAs DBR mirror and subsequently applying an electric field across such a structure provides a means of electrically tuning this group delay time. This talk will demonstrate recent progress in the design, fabrication, and characterization of such delay line structures. Various tradeoffs in device design and performance will be outlined. The benefits and drawbacks to the attempted use of such structures for generation of optical phased arrays will also be discussed.

Large Scale Spectral Hole Burning Memories In Organic Materials

Demetri Psaltis
California Institute of Technology
psaltis@caltech.edu

Persistent spectral hole burning is studied for several free-based and mettalo-naphthalocyanine derivatives in polymer hosts. These materials exhibit a strong 0-0 absorption band in region 800 nm matching the wavelength range of most semiconductor diode lasers and Ti:Sapphire lasers. Mettalo-naphthalocyanine demonstrates a nonphotochemical hole-burning mechanism that is likely related to rotations of small molecular groups, attached to a relatively rigid molecular ring. Free-base molecules exhibit a regular proton phototautomerisation mechanism of hole burning. Spectral and hole burning parameters were determined for eight materials, in particular, hole burning kinetics were analyzed and quantum efficiencies were determined to be between 0.1% and 1%. Holograms (data pages) were successfully recorded in the transmission geometry in the materials studied using single frequency laser diodes.

Optical Hole Burning Studies In Europium Doped Materials

B. R. Reddy
Alabama A&M University
Department of Physics
P.O. Box 1268
Normal, AL 35762
brreddy@aamu.edu

High-resolution spectroscopy and optical hole burning studies were performed in Y_2SiO_5: Eu^{3+} and CaF_2: Eu^{3+} at 9K and in Eu^{3+} doped oxide glass at 4K. Inhomogeneous linewidths are ~GHz in the crystals and ~6 nm in glasses. High-resolution excitation spectral recordings revealed more than forty different peaks for the $^7F_0 \rightarrow {}^5D_0$ transition of Eu^{3+} in the silicate[1] and fluoride crystals[2]. Hole burning spectra were recorded for all these different peaks, which indicated that all these satellite lines represent different sites of the dopant. Hole burning efficiencies were also measured for some transitions. The multisite behavior is due to the clustering of the dopant ions and dopant induced microscopic defects. Our studies indicate that this behavior is a universal phenomenon and is not specific to Eu^{3+} ion. However such a phenomenon is not observed in Pr^{3+} doped materials because of the strong absorption to neighboring Stark levels.

References
1. R.S.Pandher, A. Jackson, A. Davis and B. R. Reddy, "Site-selective hole burning in Eu^{3+}:Y_2SiO_5," Appl. Opt. 38, 5662 (1999).
2. R.S. Pandher, A. Davis, A. Jackson and B. R. Reddy, "High-resolution spectroscopy and optical hole burning studies of europium doped calcium fluoride," J. Appl. Phys. 87, (2000).

Fabrication and Characterization of Nano-Optic Devices

Axel Scherer
California Institute of Technology
etcher@cco.caltech.edu

We have recently developed the ability to microfabricate optical devices with feature sizes significantly smaller than the wavelength of light. Through advanced nanofabrication techniques, it is now possible to efficiently localize light and thereby miniaturize the lateral sizes of optical devices. We have designed, fabricated and tested key components necessary for making planar photonic crystal integrated circuits, such as nanocavity lasers and photonic crystal waveguides. We show that it is possible to construct lasers with photonic crystal mirrors, in which the emission wavelength, polarization and direction are all controlled entirely by the fabricated geometry of the nanocavity. We will discuss the prospects of coupling light between these lasers to form more complex networks in which light can be routed, switched and filtered within very compact photonic circuits. Finally, we will describe the possible applications of our nanocavities in the strong coupling regime, where our 0.03 cubic micron cavities are very interesting as nodes for quantum information systems.

We will also describe the development of surface plasmon enhanced light-emitting diodes, which promise to be extremely fast and efficient light emitters. Designs for our plasmon enhanced light sources combine metal-mirror vertical cavities with patterned metallic surface layers which can efficiently couple out the light from the semiconductor by exciting surface plasmons. Detailed three-dimensional electromagnetic modeling has permitted us to design and optimize the precise geometries of such devices on paper prior to microfabrication. So far, we have observed a 50-fold enhancement of the luminescence intensity over unprocessed semiconductor LED material, with clear evidence of significant Purcell enhancements in the spontaneous emission rates.

Advanced Optoelectronic Components for All-Optical Networks

Professor Jeffrey H. Shapiro
Massachusetts Institute of Technology
jshaps@mit.edu

The multidisciplinary MIT team has been working to develop key technologies and components that can substantially improve the performance, and potentially lower the cost, of future optical networks. The specific devices and subsystems that we are currently focusing on are: (1) fiber-ring and linear-fiber lasers for producing short pulses at high repetition rates for use in time-division-multiplexed (TDM) systems; (2) channel-dropping filters, based on quarter-wave shifted Bragg gratings, for use in wavelength-division-multiplexed (WDM) systems; and (3) high-index contrast photonic devices for high-density optical integration. This talk will review our recent progress in all of these areas.

Pigtailed Microresonators with Q > 1 Million

Kerry Vahala
California Institute of Technology
vahala@cco.caltech.edu

Fiber coupling to microsphere resonators having quality factors in excess of 1 million is described. Results on passive add/drop filter configurations as well as fiber-coupled microsphere lasers are presented.